AIP Journal of Applied Physics

Electron traps in organic light-emitting diodes

Min-Jan Tsai and Hsin-Fei Meng

Citation: Journal of Applied Physics **97**, 114502 (2005); doi: 10.1063/1.1913800
View online: http://dx.doi.org/10.1063/1.1913800
View Table of Contents: http://scitation.aip.org/content/aip/journal/jap/97/11?ver=pdfcov
Published by the AIP Publishing

Articles you may be interested in
Effects of interfacial stability between electron transporting layer and cathode on the degradation process of organic light-emitting diodes
Appl. Phys. Lett. **91**, 223509 (2007); 10.1063/1.2817939

Injection and transport processes in organic light emitting diodes based on a silole derivative
J. Appl. Phys. **99**, 084907 (2006); 10.1063/1.2190714

Modeling the influence of charge traps on single-layer organic light-emitting diode efficiency
J. Appl. Phys. **99**, 064509 (2006); 10.1063/1.2186374

Capacitance–voltage characterization of polymer light-emitting diodes
J. Appl. Phys. **97**, 054504 (2005); 10.1063/1.1857053

Direct observation of deep electron traps in aged organic light emitting diodes
J. Appl. Phys. **97**, 024503 (2005); 10.1063/1.1835567

Re-register for Table of Content Alerts
Create a profile.
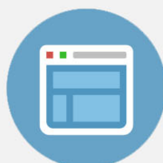
Sign up today!

[This article is copyrighted as indicated in the article. Reuse of AIP content is subject to the terms at: http://scitation.aip.org/termsconditions. Downloaded to] IP: 140.113.38.11 On: Thu, 01 May 2014 03:00:52

HTML ABSTRACT + LINKS

JOURNAL OF APPLIED PHYSICS **97**, 114502 (2005)

Electron traps in organic light-emitting diodes

Min-Jan Tsai and Hsin-Fei Meng[a)]
Institute of Physics, National Chiao Tung University, Hsinchu 300, Taiwan, Republic of China

(Received 21 October 2004; accepted 25 March 2005; published online 24 May 2005)

This work presents the effects of electron traps in organic light-emitting diodes using a model which includes charge injection, transport, and recombination. For electron-only devices, the electron current is reduced by the traps for several orders of magnitude at fixed voltage, and the traps strongly increase the transient time. For bipolar devices, due to negative trapped charges, traps enhance the hole current and the total current, opposite to the electron-only devices. The traps also make the recombination region close to the cathode. There is a voltage-dependent critical trap density beyond which the quantum efficiency decreases and transient time rises dramatically. The quantum efficiency is doubled if the hole traps are added to balance the electron and hole injections. Finally, the trap effect can be used in a bilayer light-emitting diode to make the emission color-tunable. © *2005 American Institute of Physics*. [DOI: 10.1063/1.1913800]

I. INTRODUCTION

Conjugated polymer light-emitting diode (PLED) has been of great research interest since 1990 (Ref. 1) due to its easy processing and mechanical flexibility. PLED comprises a thin layer or multilayer of intrinsic semiconducting luminescent conjugated polymer sandwiched between two electrodes. The band gap of organic semiconductor is large (>2 eV), so most charge carriers are due to injection from the electrodes. Hence, the type of electrode determines whether the device is electron-only or hole-only or bipolar. In bipolar devices carriers can move across the device and recombine to emit light. One of the most unique properties of a conjugated polymer is that the hole mobility is much higher than the electron mobility.[2,3] In fact, this mobility imbalance is expected to be the main limit for the PLED quantum efficiency. Interestingly, the imbalance measured by the time-of-flight experiment in thick devices[2] is generally much stronger than the imbalance observed by space-charge-limited current in thinner devices.[4] Because the space-charge density is inversely proportional to the square of the film thickness for fixed voltage, the apparent dependence of the imbalance on the film thickness can be attributed to the dependence of the effective electron mobility on the electron density. Such dependence suggests the presence of electron traps, which are more easily filled up in thinner devices. In our view, there are two reasons causing the higher hole mobility, both related to the electron traps. The first is that the background p-doping compensates for the hole traps caused by the structural defects; the second is that oxidation contributes to electron traps, but not to hole traps.[5] In addition to reducing the electron mobility, the electron traps may confine the electroluminescence (EL) near the cathode. Metallic electrodes are efficient quenching sites for electroluminescence, so this confinement is expected to strongly reduce the performance of the device. The imbalanced carrier mobility manifests not only in the absolute value, but also in its dependence on the electric field.[3,4] The field dependence of electron mobility exceeds that of hole mobility, and we believe that this phenomenon can also be explained by the existence of electron traps. Device models have been proposed for PLED in steady state[6,7] and transient.[8,9] Traps have also been included in some simple device model.[10,11] However, so far, very little is known for the effect of electron traps on the microscopic properties of PLED.

In this paper we present a comprehensive theoretical investigation on the effects of electron traps in polymer devices. The mobilities for free electrons and holes are assumed to be equal.[5] We employ a device model which includes explicitly the traps in the continuity equation and Poisson's equation. In the electron-only devices, higher electron trap density is shown to cause stronger field dependence of the electron current. The traps are shown not only to affect the electron transport, but also to increase dramatically the transient time required for the device to reach the steady state. For hole-only devices without traps the time scale is microsecond,[8] but in electron-only or bipolar devices the time scale can be in millisecond. For bipolar devices, the influences of traps on the recombination rate, the device efficiency, and the carrier transport are considered. It is surprising that the traps enhance the hole current due to the accumulation of a large amount of the negative space charges inside the device. As the trap density increases beyond a certain limit, the quantum efficiency drops sharply due to carrier imbalance. Interestingly, if the hole traps are added to the model to balance the electron and hole injection, the efficiency is recovered.

This paper is organized as follows: Section II discusses the device model with traps. Results and discussions for electron-only, bipolar, and bilayer devices are presented in Sec. III, and Sec. IV draws the conclusions.

II. DEVICE MODEL WITH TRAPS

In this work we assume the exponential energy distribution of traps.[10,12–14] The trap density of states has the form

[a)]Author to whom correspondence should be addressed; electronic mail: meng@faculty.nctu.edu.tw

[This article is copyrighted as indicated in the article. Reuse of AIP content is subject to the terms at: http://scitation.aip.org/termsconditions. Downloaded to] IP: 140.113.38.11 On: Thu, 01 May 2014 03:00:52

$$n_{t\varepsilon}(\varepsilon,x)=\frac{N_t(x)}{kT_t}\exp\left(\frac{(\varepsilon-\varepsilon_c)}{kT_t}\right), \tag{1}$$

where $N_t(x)$ is the trap density in position x, kT_t is the characteristic energy of traps, which is the depth of traps from the conduction band edge ε_c. The free electrons are assumed to be in thermal equilibrium with trapped electrons.[15] Using Eq. (1) and approximating the Fermi–Dirac distribution as a step function,[15] a relationship between the trapped (n_t) and free (n_f) electron density can be obtained, which is

$$n_t=N_t\left(\frac{n_f}{n_0}\right)^{T/T_t}, \tag{2}$$

where n_0 is the effective density of states for free electrons. Equation (2) is used in the continuity equation.

A. Single-layer device

In a single-layer device model, the device comprises of a thin-film layer of organic semiconductor sandwiched between two electrodes. The transport of electrons and holes are described by time-dependent continuity equations with drift-diffusion current, coupled with Poisson's equation. That is

$$\frac{\partial n_{to}}{\partial t}=\frac{1}{e}\left(\frac{\partial J_n}{\partial x}\right)+G-R, \tag{3}$$

$$\frac{\partial p}{\partial t}=-\frac{1}{e}\left(\frac{\partial J_p}{\partial x}\right)+G-R, \tag{4}$$

$$\frac{\partial E}{\partial x}=\frac{e(p-n_f-n_t)}{\epsilon}, \tag{5}$$

where

$$n_{to}=n_f+n_t, \tag{6}$$

and

$$J_n=e\mu\left(n_fE+\frac{kT}{e}\frac{\partial n_f}{\partial x}\right), \tag{7}$$

$$J_p=e\mu\left(pE-\frac{kT}{e}\frac{\partial p}{\partial x}\right). \tag{8}$$

Here, n_{to} is the total electron density, including free (n_f) and trapped (n_t) electrons. p is the hole density, J_n (J_p) is the electron (hole) current density, and G and R are the generation and recombination rate, respectively; x is the position normal to the film, and the cathode is at $x=0$; t is the time, e is the absolute electron charge, and μ is the free-carrier mobility. Note that μ is the same for electrons and holes. E is the electric field, k is Boltzmann's constant, T is the temperature, and $\epsilon=\epsilon_0\epsilon_r$ is the permittivity of the material. The diffusion coefficient is expressed in terms of the carrier mobility using Einstein's relation. Because of the large band gap of these semiconductors, the generation rate G is too small to produce enough carriers compared with injected carriers.[6,7] Therefore, G is neglected in our model. The recombination rate R is bimolecular, which takes the form[16,17]

$$R=rn_fp, \tag{9}$$

where r is Langevin recombination coefficient given by[6,7,10]

$$r=\frac{e\mu}{\epsilon}. \tag{10}$$

Substituting Eq. (2) into (3)

$$\frac{\partial n_f}{\partial t}=\frac{1}{1+B}\left(\frac{1}{e}\frac{\partial J_n}{\partial x}-rn_fp\right), \tag{11}$$

$$\frac{\partial n_t}{\partial t}=\frac{1}{1+B}\left(\frac{1}{e}\frac{\partial J_n}{\partial x}-rn_fp\right), \tag{12}$$

where

$$B=Nt\frac{T}{T_t}\left(\frac{1}{n_0}\right)^{T/T_t}\frac{1}{n_f^{1-T/T_t}}. \tag{13}$$

These equations are integrated together with the equation for the electric field[6,7]

$$\frac{\partial E(x,t)}{\partial t}=\frac{-1}{L}\frac{\partial V_L}{\partial t}-\frac{1}{\epsilon}\left[J_t(x)-\frac{1}{L}\int_0^L J_t(x)dx\right], \tag{14}$$

where V_L is the voltage at the anode, $V=0$ at the cathode, and L is the thickness of device. Equation (14) is obtained by the time derivative of Poisson's equation. Equations (11)–(14) are spatially discretized using the Scharfetter–Gummel method,[18] and the first-order differential equations are integrated forward in time. The common Poole–Frenkel form of the field dependence of the hopping mobility μ for the free carrier is used,[19–21] i.e.,

$$\mu=\mu_0\exp\left(\sqrt{\frac{E}{E_0}}\right). \tag{15}$$

A nondegenerate case is assumed when the device is in thermal equilibrium, and the carrier densities of holes and electrons are given by

$$n_f(x)=n_0\exp\left[-\left(\frac{\varepsilon_c-e\phi-\mu_c}{kT}\right)\right] \tag{16}$$

and

$$p(x)=n_0\exp\left[\left(\frac{\varepsilon_v-e\phi-\mu_c}{kT}\right)\right], \tag{17}$$

where μ_c is the chemical potential of the device in thermal equilibrium and ϕ is the potential the value of which at the left contact (cathode) is zero.

Now we discuss the boundary condition at the contacts. The thermionic emission and backflow current add up to the total current in contacts. The tunneling current is neglected because it is much smaller.[10] The anode is at the right-hand side of the device ($x=L$) and the cathode is at the opposite ($x=0$). The thermionic emission is given by

$$J_{\rm th}=AT^2e^{-\phi_b/(kT)}, \tag{18}$$

where A is Richardson's constant and ϕ_b is the energy barrier for injection from the metal to the semiconductor. The image force lowers ϕ_b in the form

[This article is copyrighted as indicated in the article. Reuse of AIP content is subject to the terms at: http://scitation.aip.org/termsconditions. Downloaded to] IP: 140.113.38.11 On: Thu, 01 May 2014 03:00:52

$$\phi_b = \phi_{b0} - e\sqrt{\frac{e|E|}{\epsilon}}, \tag{19}$$

where ϕ_{b0} is the energy barrier when the electric field is zero. The backflow current is assumed to be proportional to the carrier density near the contact. For example, the hole backflow current at the right contact is

$$J_{bf}(L) = \nu p(L). \tag{20}$$

In thermal equilibrium, the thermionic and backflow current must cancel each other, and using the hole carrier density the coefficient ν is

$$\nu = \frac{AT^2}{n_0}. \tag{21}$$

Therefore, the total hole current density at the anode is given by

$$J_p(L) = \frac{AT^2}{n_0}[p(L) - n_0 e^{-\phi_b/kT}]. \tag{22}$$

The other three currents, $J_n(0)$, $J_n(L)$, and $J_p(0)$, at the boundaries have analogous forms.

When electrons (holes) move across the device they can recombine with holes (electrons). Integrating Eq. (3) or Eq. (4) in steady state gives the recombination current J_r

$$J_r = \int_0^L eR dx = J_n(L) - J_n(0) = J_p(0) - J_p(L). \tag{23}$$

The quantum efficiency η is defined as the number of photon per charged carrier:

$$\eta = \frac{J_r}{J_t}. \tag{24}$$

$J_t = J_n + J_p$ is the total current density, which is independent of x at steady state. Here we assume that the exciton radiative decay probability is one. Both electron current at the contact for hole injection and the hole current at the contact for electron injection cause the loss of recombination efficiency η.

The initial conditions for p, n_f, n_t, and E in thermal equilibrium are obtained from Eqs. (2), (5), (16), and (17) and

$$\frac{\partial}{\partial x}\phi = -E,$$

where the relaxation method is used. The boundary conditions are the chemical potentials of the electrodes. In the time-evolution process a voltage ramp[7] is used for the first term in the right-hand side of Eq. (14), which starts from zero as the total voltage is applied. Solutions are integrated forward in time, until the total current is constant with respect to position x.

B. Bilayer device

In a bilayer device model, there are two layers of different organic semiconductors. The equations describing the carriers in each layer are the same as that for a single-layer device. The interface is designated at position x_0 with a barrier height ϕ_h for thermionic emission. In local thermal equilibrium, the hole carrier density in the left-hand side of x_o, $p(x_0^-)$ and that in the right-hand side of x_0, $p(x_0^+)$ are related by

$$\frac{p(x_0^-)}{p(x_0^+)} = \frac{n_{01}e^{-(\varepsilon_{v_1}-\mu_c)}}{n_{02}e^{-(\varepsilon_{v_2}-\mu_c)}} = \frac{n_{01}}{n_{02}}e^{-\beta\phi_h}, \tag{25}$$

where n_{01} (n_{02}) is the density of states in layer 1 (2), and ε_{v1} (ε_{v2}) is the valence-band energy in the layer 1 (2).[22] We also assume that the two layers have the same density of states such that $n_{01} = n_{02} = n_0$.

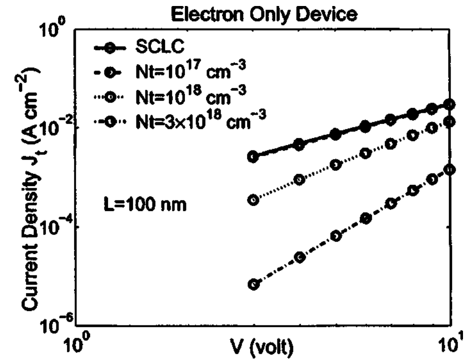

FIG. 1. Current densities as a function of applied voltage are shown with $L = 100$ nm. Electrons and holes have the same mobility of 10^{-6} cm^2 V^{-1} s^{-1}. The SCLC in Eq. (26) is presented for comparison. Trap densities $N_t = 10^{17}$ (dash), 10^{18} (short dash), and 3×10^{18} cm^{-3} (dash dot) are considered.

III. RESULTS AND DISCUSSION

The above model is applied to electron-only, bipolar, and bilayer devices. Results on the current, carrier distribution, device efficiency, and transient time are presented and discussed.

A. Electron-only device with traps

Material parameters suitable for [2-methoxy,5-(2′-ethyl-hexyloxy)-1,4-phenylene vinylene] (MEH-PPV) are used. Ca with a work function of 3.1 eV is assumed to be both the cathode and anode.[7] The conduction and valence-band energies of MEH-PPV are 2.9 and 5.3 eV, and electrons are injected from the electrode to MEH-PPV with a barrier height of 0.2 eV. The dielectric constant ϵ_r is 3, total carrier density of states n_0 is 10^{21} cm^{-3},[5] T is 300 K, and T_t is 1500 K.[10]

First, we consider the current–voltage relation with traps. In Fig. 1, current–voltage relation is plotted with trap densities $N_t = 10^{17}$, 10^{18}, and 3×10^{18} cm^{-3}, device thickness $L = 100$ nm, and $\mu_0 = 10^{-6}$ cm^2 V^{-1} s^{-1}. In order to obtain the inherent effect of traps on the field dependence of electron mobility, we assume $\mu = \mu_0$ here. For comparison the space-charge-limited current (SCLC)[15]

$$J = \frac{9}{8}\epsilon\mu\frac{V^2}{L^3} \tag{26}$$

is also plotted. At low N_t, the current–voltage relation is close to SCLC as expected. As N_t increases, electron traps not only reduce the current, but also enhance the field depen-

[This article is copyrighted as indicated in the article. Reuse of AIP content is subject to the terms at: http://scitation.aip.org/termsconditions. Downloaded to] IP: 140.113.38.11 On: Thu, 01 May 2014 03:00:52

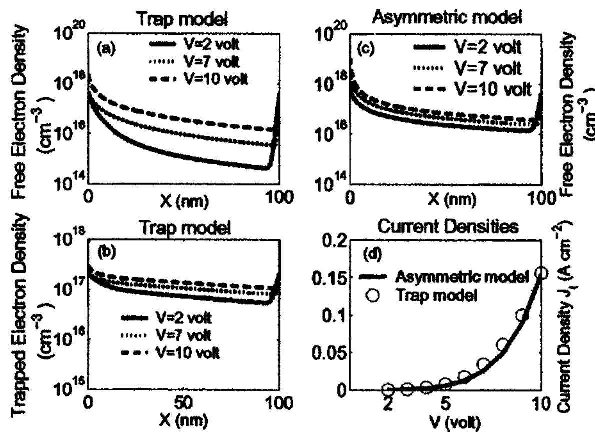

FIG. 2. (a) The free-electron densities, calculated using the trap model ($\mu_{0e}=\mu_{0h}=\mu_0$) with $\mu_0=10^{-6}$ cm^2 V^{-1} s^{-1}, $N_t=10^{18}$ cm^{-3}, and $E_0=10^5$ V cm^{-1}, are plotted. (b) The trapped electron densities calculated using parameters as those in (a). (c) The free-electron densities, calculated using the asymmetric model ($\mu_{0e}\neq\mu_{0h}$) with $\mu_{0e}=8\times10^{-11}$ cm^2 V^{-1} s^{-1} and $E_{0e}=1.9\times10^4$ V cm^{-1}, are presented. (d) The current densities calculated using the asymmetric model (line) and trap model (circle) from 2 to 10 V.

dence of electron current. The electron current approaches SCLC more as the voltage increases. The reduced magnitude and stronger field dependence of the electron current have been described alternatively by a model with an effective electron mobility but no traps.[6,7] The effective mobility is of the Poole–Frenkel form [Eq. (15)] with artificially reduced E_0 (stronger field dependence) and lower zero-field mobility μ_0 in order to describe the effect of traps. Below such description is named the asymmetry model, because the symmetry between the electron and hole mobility is explicitly broken. In Fig. 2(d) we show that the phenomenological asymmetric model and our more microscopic trap model are able to give the same current–voltage ($I-V$) curve. One then wonders whether they give the same electron distribution or not. Figure 2 plots the electron distributions calculated using different models. The free-electron distributions in Fig. 2(a) are obtained from the trap model with $N_t=10^{18}$ cm^{-3}. The trapped electron distributions are presented in Fig. 2(b) with various applied voltages. The free-electron distributions calculated without traps in the asymmetric model are shown in Fig. 2(c). The hole mobility is as before, but the electron mobility $\mu_0=8\times10^{-11}$ cm^2 V^{-1} s^{-1} and $E_0=1.9\times10^4$ V cm^{-1} are chosen to give the same $I-V$ relation. The free-electron density calculated in the trap model is much smaller than that in the asymmetry model, especially near the cathode. The smaller free-carrier density in the trap model is due to the fact that free electrons are much more mobile than those in the asymmetry model. Therefore, for a given current density much fewer electrons are needed to carry the current. This indicates that although the $I-V$ curve can be fitted very well using the asymmetry model, the carrier density predicted by such a model is incorrect. The free-electron density distribution is important for the exciton formation and quenching in bipolar devices. This suggests that any model without explicit inclusion of traps cannot be applied to the recombination and efficiency of PLED.

Next, we consider the effect of the traps on the transient time. The transient time is the real time that the device takes

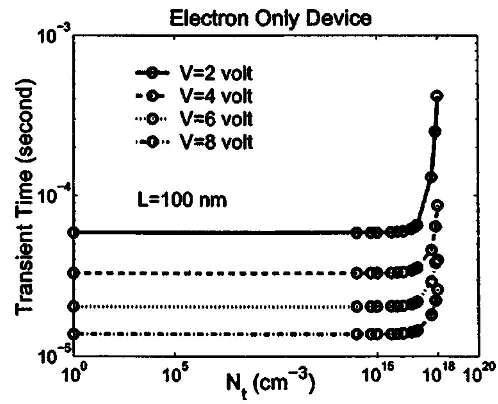

FIG. 3. The transient time with applied voltages 2, 4, 6, and 8 V is plotted against the trap density N_t. The thickness L is 100 nm. $\mu_0=10^{-6}$ cm^2 V^{-1} s^{-1} and $E_0=5\times10^5$ V cm^{-1}.

to converge to the steady state in the time evolution. Figure 3 plots the transient time versus trap density at various voltages. μ_0 is 10^{-6} cm^2 V^{-1} s^{-1}, E_0 is 5×10^5 V cm^{-1}, and L is 100 nm. As the trap density N_t increases, the electrons need more time to fill up the traps, then go throughout the device. A smaller applied voltage also causes a longer transient time because of fewer electrons to fill up the traps. As the trap density become comparable to the free-electron density, the device slows down significantly. This happens when

$$n_t=N_t\left(\frac{n_f}{n_0}\right)^{T/T_t}\simeq\frac{n_{f0}}{10}, \quad (27)$$

where n_{f0} is free-electron density in the device with zero trap density.

B. Bipolar device with traps

MEH-PPV is taken as the active layer sandwiched between the Ca and Au electrode. Au, on the right-hand side of the device, has a 0.2-eV barrier for hole injection to MEH-PPV, and the thickness of the device L is 100 nm. n_0, ϵ_r, T, and T_t are the same as those in the electron-only device.

Figure 4(a) plots the total current density as a function of the trap density N_t at 8 V. Here, $\mu_0=10^{-6}$ cm^2 V^{-1} s^{-1} and $E_0=10^5$ V cm^{-1}. The striking feature is that the current in-

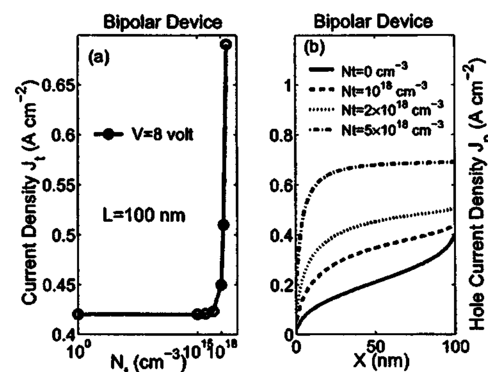

FIG. 4. (a) The current density vs trap density N_t for a bipolar device is presented with an applied voltage of 8 V. $\mu_0=10^{-6}$ cm^2 V^{-1} s^{-1}, $E_0=10^5$ V cm^{-1}, and $L=100$ nm. (b) The hole current density distributions are plotted with trap densities 0, 10^{18}, 2×10^{18}, and 5×10^{18} cm^{-3}. The hole injection at the anode ($x=100$ nm) increases with trap density.

[This article is copyrighted as indicated in the article. Reuse of AIP content is subject to the terms at: http://scitation.aip.org/termsconditions. Downloaded to] IP: 140.113.38.11 On: Thu, 01 May 2014 03:00:52

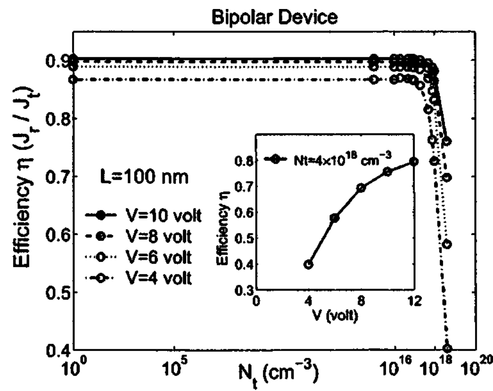

FIG. 5. The quantum efficiency η vs trap density N_t is presented in applied voltages 4, 6, 8, and 10 V. $\mu_0=10^{-6}$ cm^2 V^{-1} s^{-1}, $E_0=5\times10^5$ V cm^{-1}, and device thickness $L=100$ nm. The inset shows the relation between efficiency and applied voltage.

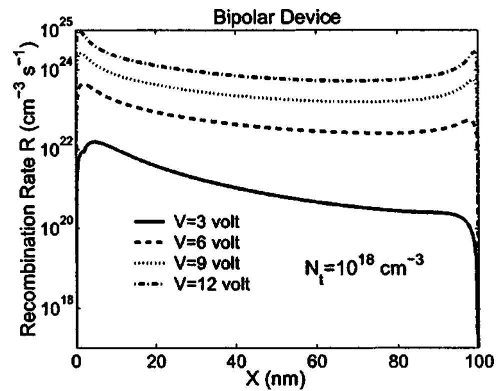

FIG. 7. The distributions of recombination rate are presented with applied voltages 3, 6, 9, and 12 V. The trap density of 10^{18} cm^{-3} is used. $\mu_0=10^{-6}$ cm^2 V^{-1} s^{-1} and $E_0=10^5$ V cm^{-1}.

creases with N_t, contrary to what intuition would suggest. In electron-only devices, some electrons are trapped so that the electron current declines when the trap density N_t increases. In bipolar devices, however, the trapped electrons increase the total negative space charge, which enhances the hole injection by Coulomb attraction, as illustrated in Fig. 4(b). The hole current density J_p presented in Fig. 4(b) increases with the trap density, causing a larger total current density.

The PLED efficiency η is shown in Fig. 5 as a function of the trap density N_t and the applied voltage. When N_t increases, the efficiency declines faster at a smaller voltage than that at a higher voltage, suggesting that the imbalance between the electron and hole current in the device with a smaller voltage exceeds that in the device at a higher voltage. This is consistent with Fig. 1, where *IV* approaches SCLC with increasing voltage. There are also critical trap densities in Fig. 5, determined by Eq. (27) as before. For fixed N_t, the efficiency of the device increases with the applied voltage since the traps are more filled up and the electron-hole injection is more balanced, as shown in the inset.

The distribution of the recombination R is important in PLED, since the dominant light-generation zone determines how serious the cathode quenching effect is. Figure 6 plots the recombination distribution through the device. The recombination distribution is symmetrical when $N_t=0$, and the main recombination zone approaches the cathode as N_t increases. Also, the absolute value of recombination itself increases with the trap density near the cathode due to the increased density of holes, attracted toward the cathode by the trapped negative space charge. Clearly, the electron traps detrimentally affect the luminescence efficiency, since most excitons are quenched by the cathode plasma mode. Figure 7 plots the distribution of the recombination rate R with $N_t=10^{18}$ cm^{-3} at various voltages. The figure shows that applying a higher voltage pushes the electrons away from the cathode to the anode, smoothing the distribution and reducing the cathode quenching. So at higher voltage, not only is the carrier injection more balanced, as shown in Fig. 5, but also the cathode quenching is reduced. Both factors contribute to the increasing efficiency with voltage.

The transient time for the bipolar device is shown in Fig. 8. The device at high voltage needs less time to reach the steady state because the traps are filled rapidly as the picture in the electron-only device. For a lower voltage, the transient time could be as slow as a millisecond. Note that such a long transient time is not possible in the asymmetry model without traps.[8] Because the build-in potential in the bipolar device is larger than that in the electron-only device where electrons move faster, the transient time required for bipolar devices is longer than that for electron-only devices.

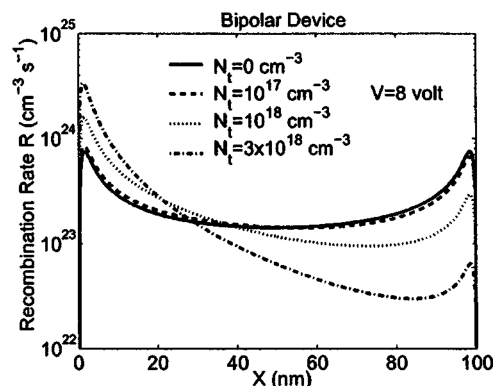

FIG. 6. The distributions of recombination rate are plotted at 8 V. The recombination rate is shown for $N_t=0$, 10^{17}, 10^{18}, and 3×10^{18} cm^{-3}. $\mu_0=10^{-6}$ cm^2 V^{-1} s^{-1} and $E_0=10^5$ V cm^{-1}.

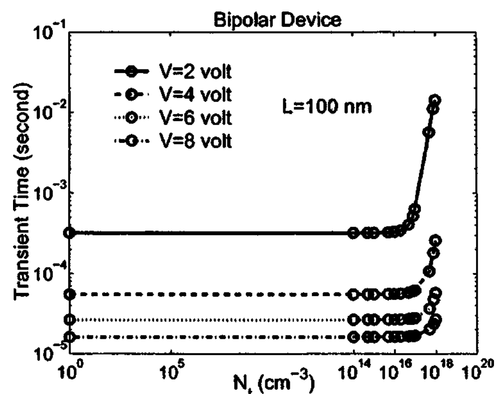

FIG. 8. The transient time of a bipolar device vs trap density is shown. Here, $\mu_0=10^{-6}$ cm^2 V^{-1} s^{-1} and $E_0=5\times10^5$ V cm^{-1}. The device thickness is $L=100$ nm.

[This article is copyrighted as indicated in the article. Reuse of AIP content is subject to the terms at: http://scitation.aip.org/termsconditions. Downloaded to] IP: 140.113.38.11 On: Thu, 01 May 2014 03:00:52

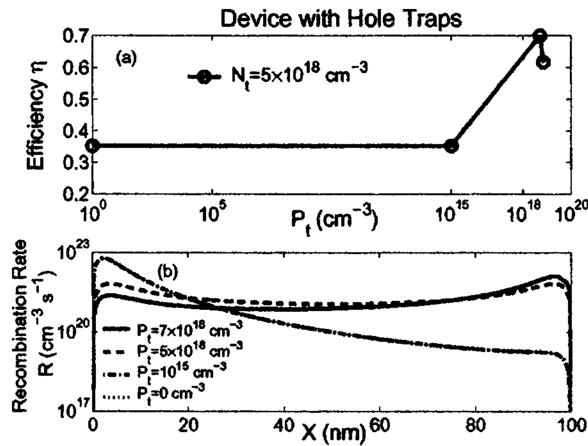

FIG. 9. (a) Efficiency vs hole trap density is shown for the electron trap density $N_t=5\times10^{18}$ cm^{-3} at 4 V. The hole trap densities P_t are 0, 10^{15}, 5×10^{18}, and 7×10^{18} cm^{-3}. $\mu_0=10^{-6}$ cm^2 V^{-1} s^{-1} and $E_0=10^5$ V cm^{-1}. (b) The recombination rate vs position is presented with the same parameters. The recombination is symmetrical when the hole and electron trap densities are the same, corresponding to a maximum value of the efficiency.

Electron traps are inevitable as discussed in the Introduction. After showing their adverse effect on the PLED efficiency, one may wonder if such an effect can be cured. One promising idea is to introduce hole traps into the semiconductor.[23] The hole traps are supposed to balance the carrier injection and increase the luminescent efficiency. Figure 9(a) presents the efficiency for a device with an electron trap density of $N_t=5\times10^{18}$ cm^{-3} at 4 V. As the hole trap density P_t is zero, $\eta=0.35$ due to the imbalance. As P_t increases, the efficiency is indeed enhanced and doubled from 0.35 to 0.7 when $P_t=5\times10^{18}$ cm^{-3}, where the recombination distribution is symmetrical. Increasing the number of hole traps beyond the electron trap density ($P_t=7\times10^{18}$ cm^{-3}) diminishes the efficiency of the device, since the imbalance of carriers comes back. Hole traps also contribute to the fall in quenching, since the recombination rate is made smoother, as shown in Fig. 9(b).

C. Bilayer device

One of the most remarkable effects of the traps on the recombination distribution is that the recombination concentrates near the cathode at low voltage and spreads out to the whole device at higher voltage (Fig. 7). Although such a spread in recombination does not change the emission spectrum for single-layer PLED, it suggests the possibility of

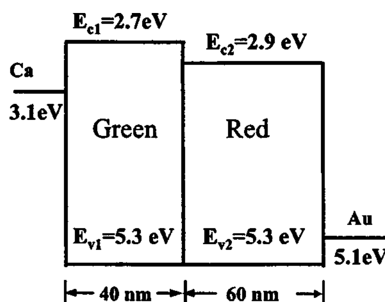

FIG. 10. The scheme of a bilayer device is shown. Layer thicknesses and band energies are indicated.

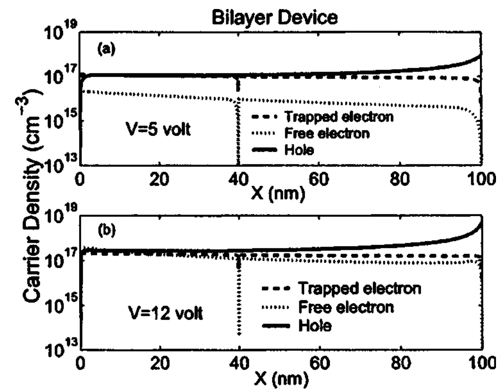

FIG. 11. The carrier density distribution of holes, free electrons, and trapped electrons are shown in the bilayer device (Fig. 10) at 5 and 12 V. $\mu_0=10^{-6}$ cm^2 V^{-1} s^{-1} and $E_0=5\times10^5$ V cm^{-1}.

continuous color tuning by voltage in PLED with two emissive layers. Below we study a bilayer device with electron traps. In our device a green emissive layer next to the cathode has a conduction-band energy E_c of 2.7 eV and a valence-band energy E_v of 5.3 eV, with a thickness of 40 nm. The layer next to the anode is the red-emissive MEH-PPV, with a thickness of 60 nm. The device is sandwiched between Ca and Au electrodes, and the electron trap density in each layer is 10^{18} cm^{-3}; $\mu_0=10^{-6}$ cm^2 V^{-1} s^{-1}, $E_0=5\times10^5$ V cm^{-1}, $n_0=10^{21}$ cm^{-3}, and T and T_t are 300 and 1500 K. Figure 10 schematically depicts the bilayer device. Figure 11 shows the carrier densities of holes, free electrons, and trapped electrons at 5 V in the upper panel and 12 V in the lower panel. The shape of the hole distribution is quite uniform and does not depend on the voltage much. On the other hand, the electron density concentrates in the green layer at 5 V and becomes uniform at 12 V. The recombination rate is shown in Fig. 12 at 5 and 12 V. As expected, the recombination in the red layer relative to the green layer increases significantly with voltage, resulting in a color tuning.

IV. CONCLUSION

Many experiments have demonstrated the imbalance of holes and electrons. We show here that all the observed results can be captured by the electron trap model with sym-

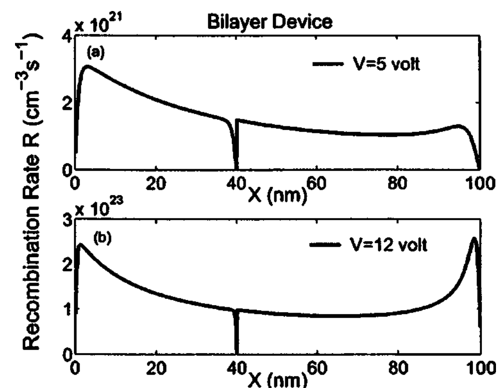

FIG. 12. Recombination rate vs position is shown with the applied voltage of 5 V in (a) and 12 V in (b). Parameters are the same as that in Fig. 11.

[This article is copyrighted as indicated in the article. Reuse of AIP content is subject to the terms at: http://scitation.aip.org/termsconditions. Downloaded to] IP: 140.113.38.11 On: Thu, 01 May 2014 03:00:52

metric free-carrier mobilities. Although the asymmetry model, in which the imbalance is described by artificially breaking the mobility symmetry, can fit the current–voltage curve accurately, the predicted electron density significantly exceeds that calculated in the more microscopic trap model. The model without explicit consideration of traps is therefore inappropriate for discussing the device recombination rate or efficiency. Traps affect not only the current and recombination, but also the transient time required for the device to reach the steady state. A time scale of millisecond arises in bipolar devices with higher trap density. In PLED, traps cause the recombination zone to approach the cathode, seriously affecting the device luminescence and efficiency due to the metal quenching. Addition of hole traps recovers the balance of carrier densities and doubles the efficiency. Our works show that almost all transport and electroluminescence properties of organic devices are determined by the electron traps, and the control of such traps is the key to improve the PLED efficiency.

ACKNOWLEDGMENTS

This work was supported by the National Science Council of the Republic of China under Grant No. NSC89-2112-M009-047 and the Excellence Project Semiconducting Polymers for Electroluminescence under Grant No. 91-E-FAO4-2-4A of the ROC Ministry of Education.

[1] J. H. Burroughes, D. D. C. Bradley, A. R. Brown, R. N. Marks, K. Mackey, R. H. Friend, P. L. Burn, and A. B. Holmes, Nature (London) **347**, 539 (1990).
[2] H. Antoniades, M. A. Abkowitz, and B. R. Hsieh, Appl. Phys. Lett. **65**, 2030 (1994).
[3] P. W. M. Blom and M. C. J. M. Vissenberg, Mater. Sci. Eng., R. **27**, 53 (2000).
[4] L. Bozano, S. A. Carter, J. C. Scott, G. G. Malliaras, and P. J. Brock, Appl. Phys. Lett. **74**, 1132 (1999).
[5] H. F. Meng and Y. S. Chen, Phys. Rev. B **70**, 115208 (2004).
[6] B. K. Crone, P. S. Davids, I. H. Campbell, and D. L. Smith, J. Appl. Phys. **84**, 833 (1998).
[7] P. S. Davids, I. H. Campbell, and D. L. Smith, J. Appl. Phys. **82**, 12 (1997).
[8] D. J. Pinner, R. H. Friend, and N. Tessler, J. Appl. Phys. **86**, 5116 (1999).
[9] B. Ruhstaller, S. A. Carter, S. Barth, H. Riel, W. Riess, and J. C. Scott, J. Appl. Phys. **89**, 4575 (2001).
[10] P. W. M. Blom and M. J. M. de Jong, IEEE J. Sel. Top. Quantum Electron. **4**, 105 (1998).
[11] C. D. J. Blades and A. B. Walker, Synth. Met. **111–112**, 335 (2000).
[12] A. J. Campbell, D. D. C. Bradley, and D. G. Lidzey, J. Appl. Phys. **82**, 6326 (1997).
[13] P. E. Burrows, Z. Shen, V. Bulovic, D. M. McCarty, S. R. Forrest, J. A. Cronin, and M. E. Thompson, J. Appl. Phys. **79**, 7991 (1996).
[14] K. C. Kao and W. Hwang, *Electrical Transport in Solids* (Pergamon, Oxford, 1981).
[15] M. A. Lampert and P. Mark, *Current Injection in Solids* (Academic, New York, 1970).
[16] P. W. M. Blom, M. J. M. de Jong, and S. Breekijk, Appl. Phys. Lett. **71**, 930 (1997).
[17] V. N. Abadumov, V. I. Perel, and I. N. Yassievich, *Nonradiative Recombination in Semiconductors* (North-Holland, Amsterdam, 1991), p. 10.
[18] D. L. Scharfetter and H. K. Gummel, IEEE Trans. Electron Devices **ED-16**, 64 (1969).
[19] H. Bässler, Phys. Status Solidi B **175**, 15 (1993).
[20] Y. N. Gartstein and E. M. Conwell, Chem. Phys. Lett. **245**, 351 (1995).
[21] D. H. Dunlap, P. E. Parris, and V. M. Kenkre, Phys. Rev. Lett. **77**, 542 (1996).
[22] B. K. Crone, P. S. Davids, I. H. Campbell, and D. L. Smith, J. Appl. Phys. **87**, 1974 (2000).
[23] A. J. Campell, D. D. C. Bradley, T. Virgili, D. G. Lidzey, and H. Antoniadis, Appl. Phys. Lett. **79**, 3872 (2001).

[This article is copyrighted as indicated in the article. Reuse of AIP content is subject to the terms at: http://scitation.aip.org/termsconditions. Downloaded to] IP: 140.113.38.11 On: Thu, 01 May 2014 03:00:52